Latent Heating Contribution from Precipitation Systems with Different Sizes, Depths, and Intensities in the Tropics

CHUNTAO LIU

Department of Physical and Environmental Sciences, Texas A&M University–Corpus Christi, Corpus Christi, Texas

SHOICHI SHIGE

Graduate School of Science, Kyoto University, Kyoto, Japan

YUKARI N. TAKAYABU

Atmosphere and Ocean Research Institute, Tokyo University, Tokyo, Japan

EDWARD ZIPSER

Department of Atmospheric Sciences, University of Utah, Salt Lake City, Utah

(Manuscript received 25 May 2014, in final form 17 September 2014)

ABSTRACT

Latent heating (LH) from precipitation systems with different sizes, depths, and convective intensities is quantified with 15 years of LH retrievals from version 7 Precipitation Radar (PR) products of the Tropical Rainfall Measuring Mission (TRMM). Organized precipitation systems, such as mesoscale convective systems (MCSs; precipitation area $> 2000\,km^2$), contribute to 88% of the LH above 7 km over tropical land and 95% over tropical oceans. LH over tropical land is mainly from convective precipitation, and has one vertical mode with a peak from 4 to 7 km. There are two vertical modes of LH over tropical oceans. The shallow mode from about 1 to 4 km results from small, shallow, and weak precipitation systems, and partially from congestus clouds with radar echo top between 5 and 8 km. The deep mode from 5 to 9 km is mainly from stratiform precipitation in MCSs.

MCSs of different regions and seasons have different LH vertical structure mainly due to the different proportion of stratiform precipitation. MCSs over ocean have a larger fraction of stratiform precipitation and a top-heavy LH structure. MCSs over land have a higher percentage of convective versus stratiform precipitation, which results in a relatively lower-level peak in LH compared to MCSs over the ocean. MCSs during monsoons have properties of LH in between those typical land and oceanic MCSs.

Consistent with the diurnal variation of precipitation, tropical land has a stronger LH diurnal variation than tropical oceans with peak LH in the late afternoon. Over tropical oceans in the early morning, the shallow mode of LH peaks slightly earlier than the deep mode. There are almost no diurnal changes of MCSs LH over oceans. However, the small convective systems over land contribute a significant amount of LH at all vertical levels in the afternoon, when the contribution of MCSs is small.

1. Introduction

Latent heating (LH) release from precipitation processes in the tropics plays an important role in driving the global atmospheric circulation (Riehl and Malkus 1958). Therefore, it is critical to correctly describe the LH from subgrid-scale clouds in climate models (Arakawa 1975). Because of the large variety of cloud and precipitation processes in the tropics, the vertical profiles of LH in different regions and seasons may change significantly (Nitta and Esbensen 1974; Thompson et al. 1979; Frank and McBride 1989). Because of different microphysical processes, LH profiles from convective and

Corresponding author address: Dr. Chuntao Liu, Department of Physical and Environmental Sciences, Texas A&M University–Corpus Christi, 6300 Ocean Dr., Corpus Christi, TX 78412-5892.
E-mail: chuntao.liu@tamucc.edu

DOI: 10.1175/JCLI-D-14-00370.1

stratiform precipitation have been shown to have distinct vertical structures (Houze 1989) and could have different impacts on controlling large-scale circulation (Emanuel et al. 1994; Schumacher et al. 2004). Deep and shallow precipitation systems may contribute to different atmospheric circulation responses as well (Takayabu et al. 2010). Therefore, it is important to quantify the LH of different types of rainfall systems in the tropics.

In practice, LH is difficult to measure. Yanai et al. (1973) proposed a way to relate the unresolved diabatic processes in the atmosphere including LH from coarse sounding networks to the large-scale circulation. The apparent heating Q_1 from the unresolved diabatic processes can be defined as

$$Q_1 = \frac{\partial \overline{s}}{\partial t} + \overline{v} \cdot \nabla \overline{s} + \omega \frac{\partial \overline{s}}{\partial p} = Q_R + L_v(c - e) + L_f(f - m) + L_s(d - s_{\text{sub}}) - \left(\nabla \cdot \overline{s'v'} + \frac{\partial \overline{s'\omega'}}{\partial p} \right), \quad (1)$$

where $s = C_pT + gz$ is the dry static energy; Q_R is the atmospheric radiative heating or cooling; $L_v(c - e) + L_f(f - m) + L_s(d - s_{\text{sub}})$ is LH including condensation, evaporation, freezing of raindrops, melting of snow and graupel, deposition of ice particles, and sublimation of ice particles; and $\nabla \cdot \overline{s'v'} + (\partial \overline{s'\omega'}/\partial p)$ is the eddy transport of sensible heat. Assuming that LH is a dominant term in Eq. (1) in precipitation systems, LH can be roughly estimated with the residual of thermodynamic measurements from sounding networks (Yanai et al. 1973; Johnson 1976; Yanai and Johnson 1993). Since then, estimating the LH from enhanced sounding network has been one objective in various field campaigns (Johnson 1984; Mapes et al. 2003; Schumacher et al. 2007). However, because of the cost, the field campaigns can only provide LH estimates over limited regions during specific time periods.

An alternative way to estimate LH is from satellite observations. The Tropical Rainfall Measuring Mission (TRMM; Simpson et al. 1988; Kummerow et al. 1998) was launched in late 1997 with one of its major goals to provide tropical LH estimates. By combining cloud-resolving model simulations and the properties of cloud and precipitation indicated by TRMM Precipitation Radar (PR) and Microwave Imager (TMI) observations, LH profiles may be derived reasonably with global coverage (Tao et al. 2006). Using these LH estimates, there have been many studies on the variability of LH at different space and time scales, such as the Madden–Julian oscillation (Morita et al. 2006; Zhang et al. 2010), El Niño (Schumacher et al. 2004; Tao et al. 2006; Shige et al. 2007, 2008), and the temporal variation of heating profiles associated with isolated cold cloud systems (Imaoka and Nakamura 2013). The relationships between LH and precipitation intensity have also been discussed (e.g., Schumacher et al. 2007; Tao et al. 2010). However, there is still lack of a detailed study to quantify the vertical structure of LH from the various types of precipitation systems. To be able to correctly describe the LH effects in climate models, it is important to understand how LH changes with different types of precipitation systems and their life cycles. For example, it is well known that an isolated convective system would likely have a bottom-heavy LH profile only from convective precipitation. But a mature mesoscale convective system (MCS) could have a top-heavy LH profile from a large region of stratiform precipitation (Houze 2004; Jakob and Schumacher 2008). How to quantitatively describe LH vertical distribution in climate models could be critical to produce a correct general circulation response. The purpose of this paper is to quantify the contribution of LH from precipitation systems of various types and provide a foundation to validate climate models from a precipitation system organization perspective. The main questions addressed include the following:

- What is the contribution of LH at different vertical levels by organized precipitation systems of various sizes, depths, and intensities?
- How do organized precipitation systems vary across regions and how would that lead to different vertical structures of LH?
- What are the diurnal variations of LH at different vertical levels over tropical land and ocean? What are the roles of organized convection in the diurnal variation of LH?

To answer the above questions, LH retrievals from 15 years of TRMM PR are analyzed to budget the contributions of LH from precipitation systems with different horizontal extents, depths, and convective intensities. The diurnal variations of the LH vertical structure are analyzed and the contributions from organized precipitation systems are estimated over land and ocean separately.

2. Data and methodology

Several different methods of deriving LH from TRMM observations have been developed by various research groups based on different TRMM observation inputs (Tao et al. 2006). We choose the retrievals of the spectral latent heating (SLH) algorithm (Shige et al. 2004) in the current study. The SLH algorithm retrieves

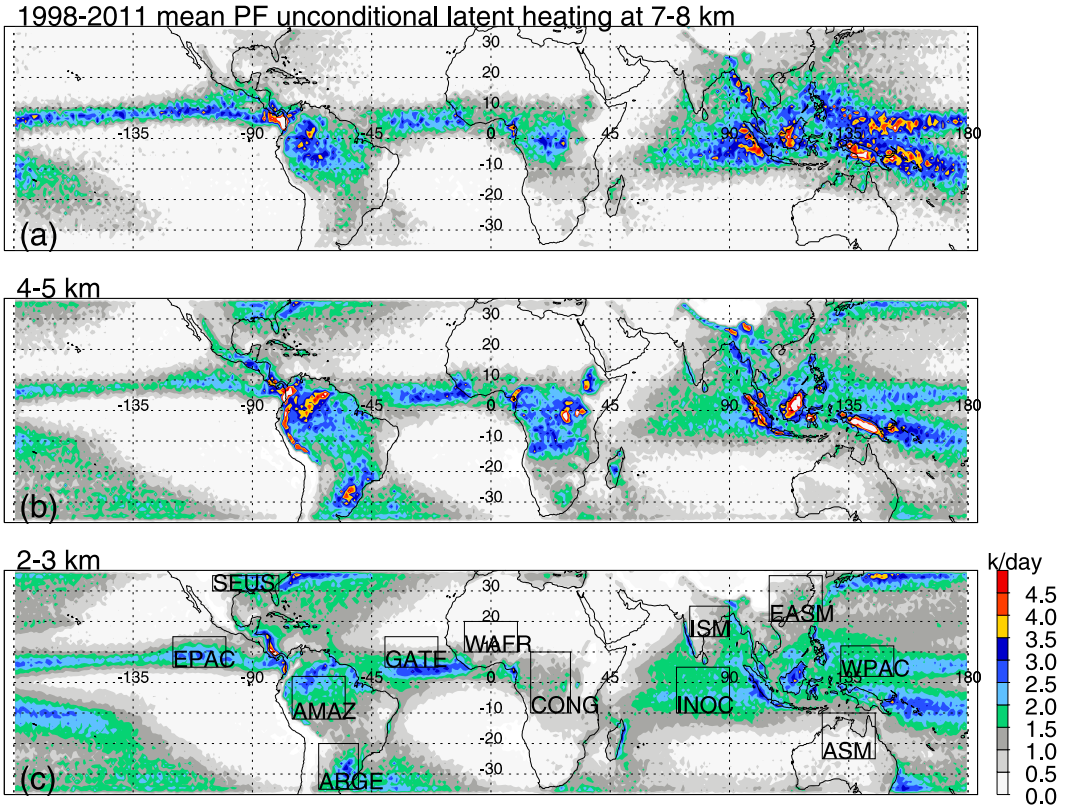

FIG. 1. Global geographical distribution of the mean unconditional LH at (a) 7–8-, (b) 4–5-, and (c) 2–3-km levels from Precipitation Features during 1998–2011. This analysis is similar to Tao et al. (2006, their Fig. 1) except from accumulation of LH from precipitation features instead of from pixels. Note that several regions of interest are shown with boxes in (c) and discussed in section 3 and Table 2.

LH from TRMM PR observations based on a lookup table built from cloud-resolving simulations. With the TRMM PR–derived radar echo-top height, precipitation rate at the near-surface level as well as at the freezing level, and partition of regions with convective and stratiform precipitation, mean LH vertical profiles are selected by matching radar profiles derived from cloud-resolving model simulations (Shige et al. 2004). This approach could have large uncertainties in the individual instantaneous LH profiles due to the timing mismatches between the water phase change process and the presence of the large hydrometeors detectable by radar. However, these retrievals successfully utilize constraints from radar observables and may provide reasonable LH vertical structures in a statistical sense (Shige et al. 2009; Takayabu et al. 2010). Details of the SLH retrieval algorithm are described in Shige et al. (2004, 2007, 2008, 2009).

There are several caveats in using the SLH retrievals. One key to correctly deriving the total LH is the partition of convective and stratiform precipitation (Houze 1997). The PR partitioning algorithm relies on the horizontal and vertical gradient of radar reflectivity (Awaka et al. 1998, 2009). There are some known difficulties of the algorithm for isolated shallow systems (Schumacher and Houze 2003; Funk and Schumacher 2013) and those over high terrain (Fu and Liu 2007). In some special scenarios, stratiform and convective partitioning could be difficult. For example, convective precipitation due to terrain lifting and in tropical cyclones could possibly be misidentified as stratiform with a top-heavy LH profile when there is little evaporation of rain in a moist lower troposphere. The SLH algorithm relies on cloud-resolving model simulations to build its lookup table. As of this writing, no simulations of strong continental convection have been used to create lookup tables. Directly using the product from the SLH algorithm over some land areas could be problematic. The above issues could introduce some uncertainties to the vertical distribution of the LH. Because the total LH is directly constrained by the precipitation rate and convective versus stratiform partition, uncertainties in the spectrum of LH contributions from precipitation systems of different size, depth, and convective intensity over land are expected. However, further study is needed to estimate how such uncertainties as these could impact our analysis.

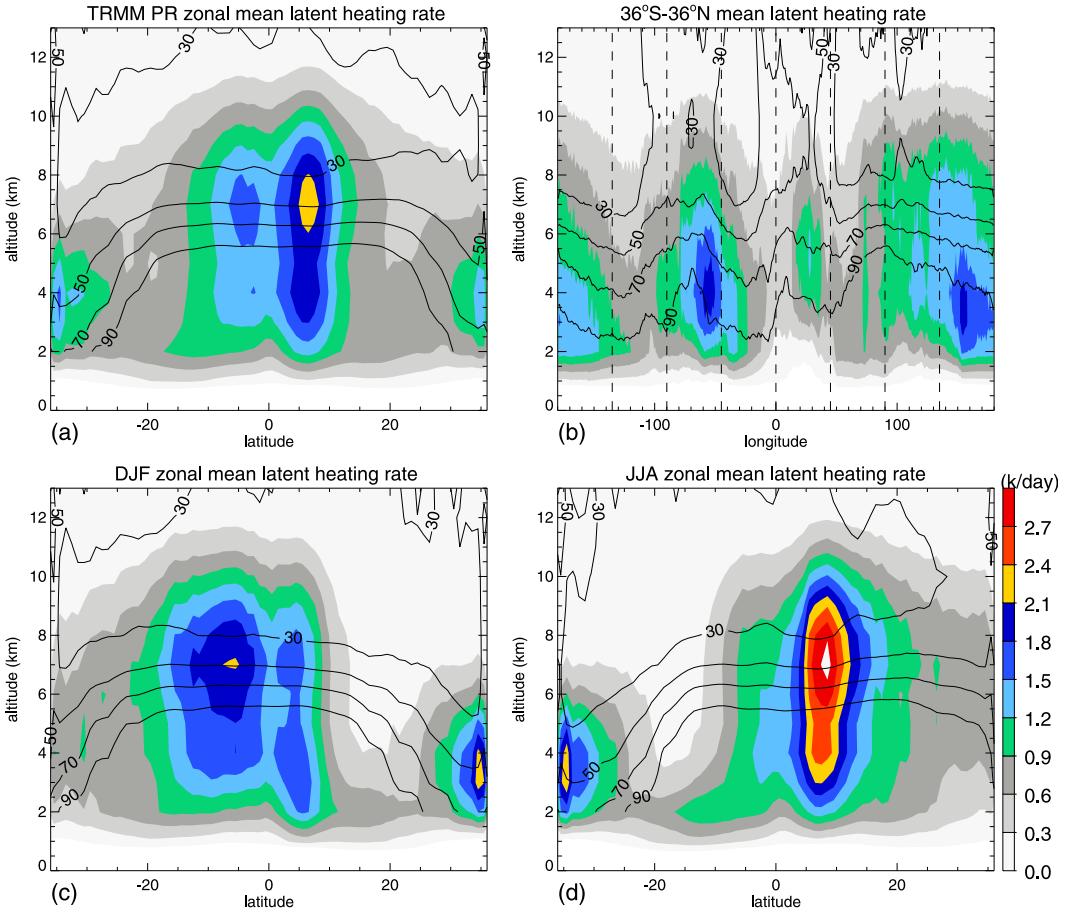

FIG. 2. (a) Mean unconditional LH rate at different latitudes and altitudes (color fill) and percent of heating from the convective precipitation (contours) from precipitation features during 1998–2011. (b) As in (a), but for LH rate at different longitudes. (c) As in (a), but during December–February. (d) As in (a), but during June–August.

To examine the contribution of LH from precipitation systems of different properties, the TRMM Precipitation Feature (PF) database (Liu et al. 2008) is used. First, the PFs are defined by grouping the area with any PR detectable echoes in the column from 15 years of TRMM observations during 1998–2012. This definition includes thick anvil regions with radar echo aloft but without detectable surface precipitation. The properties of the each PF, such as geometric center, size, maximum echo-top height, and convective intensity proxies including lightning counts and maximum 30-dBZ echo-top height, are summarized from the TRMM PR and Lightning Imaging Sensor (LIS) observations. Then the total volumetric LH at 19 different vertical levels in the stratiform and convective regions of each PF are calculated from SLH retrievals in version 7 TRMM 2H25 products (Shige et al. 2009). There are more than 113 million PFs defined from 15 years of observations. Note that because of the sensitivity of the TRMM PR, limited to reflectivities >17–18 dBZ, some weak precipitation, such as drizzle in stratocumulus or showers that fill only a small fraction of the PR's 20-km^2 footprint, are not detected (Lebsock and L'Ecuyer 2011). Although this weak precipitation is not included, the PF samples used in this study contribute the majority (~90%) of precipitation and LH in the tropics and subtropics.

3. Results

a. General climatology of LH in the tropics

The geographical distributions of the unconditional LH (mean latent heating rate including all precipitation rates including zero) are calculated by summing the total LH from PFs with a geometric center in each 1° × 1° box, and then dividing by the total number of samples. As shown in Fig. 1, the unconditional LH at three different vertical levels is similar to the climatology generated from pixel-level data (Tao et al. 2006, their Fig. 1). The LH is greater at higher altitudes (Figs. 1a,b) than at lower altitudes (Fig. 1c), and stronger in the tropics than

TABLE 1. Contributions of LH from PFs with different size, depth, and intensity over tropical land and oceans.

	Tropical land (20°S–20°N)			Tropical ocean (20°S–20°N)		
Percent of LH from PFs (%)	2–5 km	5–7 km	>7 km	2–5 km	5–7 km	>7 km
Area <400 km^2	15	6	2.5	21	2.8	0.5
Area 400–2000 km^2	23	16	9.5	23	10.2	4.5
Area > 2000 km^2	62	78	88	56	87	95
Area > 10 000 km^2	36	52	65	35	68	81
Echo top < 5 km	4	0	0	13	0	0
Echo top 5–10 km	26	18	7	30	16	7
Echo top > 10 km	70	82	93	57	84	93
30-dBZ top < 4	5	1	0.2	16	0.3	0.2
30-dBZ top 4–7 km	28	22	16.8	38	33	27.8
30-dBZ top > 7 km	67	77	83	46	66.7	72
With lightning	57	66	71	18	26	27

the subtropics with large regional variations. This is also demonstrated with the zonal means of LH in Fig. 2. On average, LH is greater north of equator with deeper heating in the tropics than subtropics (Fig. 2a). In the tropics, there are two dominant modes of LH, with a relatively weaker mode at 2–4 km and stronger heating at 6–8 km, which is consistent with past literature (Shige et al. 2009; Takayabu et al. 2010). The LH from convective precipitation dominates (>90%) at levels below 5 km in the tropics (Fig. 2a). There are large longitudinal variations of total LH, as well as of the fractional contribution from convective precipitation (Fig. 2b). Similar to Fig. 4c of Schumacher et al. (2004), the high convective fraction of LH corresponds mostly to major

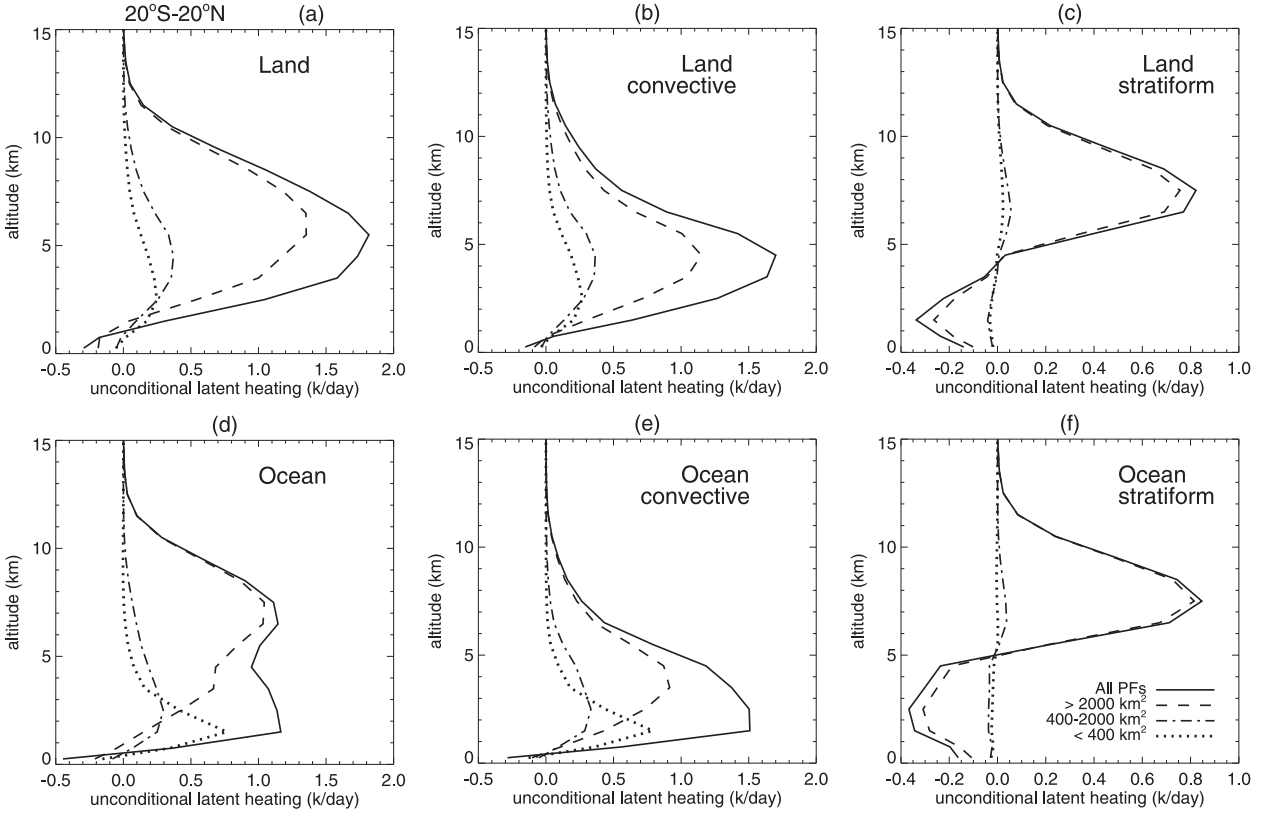

FIG. 3. (a) Mean unconditional LH and contribution from the precipitation features with different area sizes over tropical (20°S–20°N) land. (b) As in (a), but for LH from the convective precipitation in PFs. (c) As in (a), but for LH from stratiform precipitation in PFs. (d)–(f) As in (a)–(c), but for tropical ocean. Note that PFs with 1–3 pixels are included in this analysis. Solid, dashed, dash-dotted, and dotted lines represent all PFs, PFs with areas greater than 2000 km^2, PFs with areas between 400 km^2 and 2000 km^2, and PFs with areas less than 400 km^2, respectively.

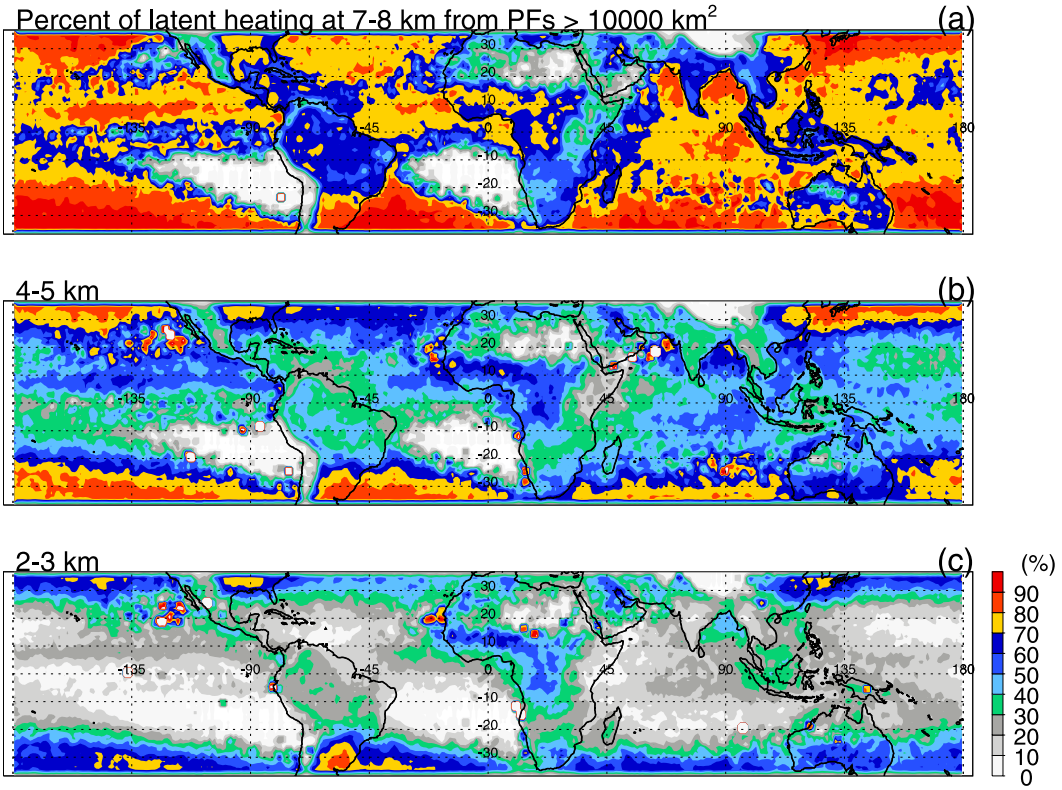

FIG. 4. (a) Percent of LH contribution at 7–8-km level from the precipitation features larger than 10 000 km^2. (b) As in (a), but at 4–5-km level. (c) As in (a), but at 2–3-km level.

continents, but also extends from Asia into the Pacific Ocean. The vertical structure of LH also changes significantly in different seasons. In December–February, LH is slightly stronger and deeper south of the equator (Fig. 2c). In July–August, LH is mainly to the north of the equator. It is interesting that there is a strong shallow LH region over the subtropics during the winter months with a large fraction of LH from stratiform precipitation (Figs. 2c,d). All these regional and seasonal variations of LH vertical structures are directly tied to the variations of precipitation and the properties of precipitation systems.

b. *Contribution from precipitation systems with different sizes*

In recent years, it has been realized that correctly describing the development of organized convective systems is one of the major challenges of climate models (Del Genio 2012; Mapes and Neale 2011). The importance of organized convection to LH is directly indicated by the dominant precipitation contribution from MCS (Nesbitt et al. 2006; Liu 2011). Further, because of the top-heavy structure of LH in the stratiform-rich precipitation region (Houze 1989), MCSs have a larger contribution to the heating at higher altitudes from large areas of stratiform precipitation than those from isolated deep convection, especially over oceans. This is evident from the dominant contributions of LH above 7 km from MCSs (PFs with area greater than 2000 km) as listed in Table 1. In fact, MCSs contribute more than half of all LH at all levels above 2 km over both land and ocean.

Figure 3 shows the unconditional LH rate over tropical land and ocean derived from PFs of various sizes over regions with convective and stratiform precipitation. Similar to the results of Takayabu et al. (2010, Fig. 1), over tropical land, the total unconditional LH maximizes between 4 and 7 km (Fig. 3a). This stems from a combination of a larger proportion of LH at 3–5 km in the convective region (Fig. 3b) and a smaller proportion of LH above 6–9 km in the stratiform region (Fig. 3c). The contribution of the MCSs is dominant at all levels in both convective (Fig. 3b) and stratiform regions (Fig. 3c). Smaller PFs (<400 km^2) contribute a small portion of the LH at 3–7 km. Over tropical oceans, consistent with Takayabu et al. (2010), there are shallow and deep modes of LH (Fig. 3d). Small PFs (<400 km^2) contribute a large portion of LH below 3 km in the form of convective precipitation. Most of these small systems are shallow and dominated by the warm

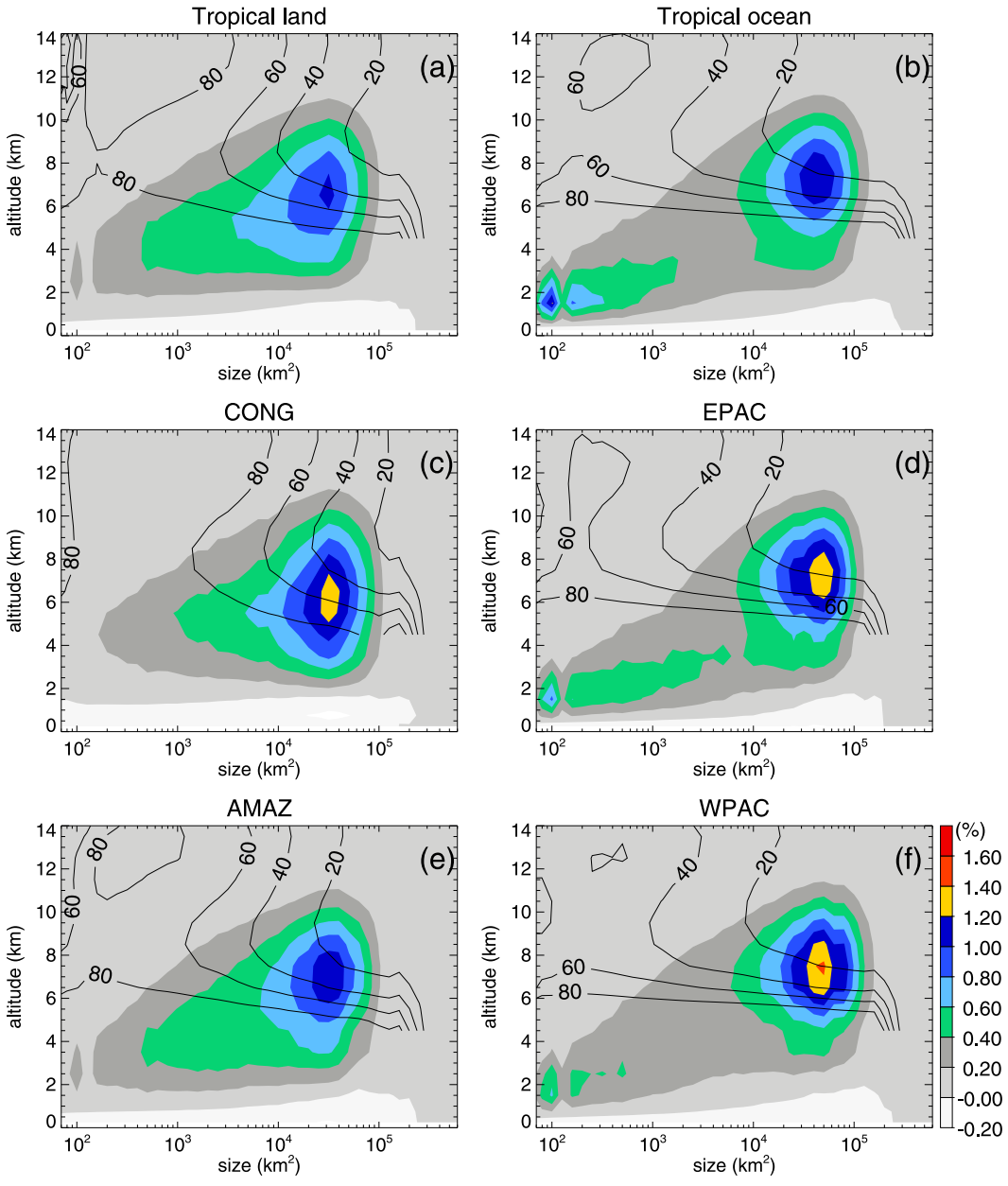

FIG. 5. Fractional contribution to LH at different altitudes from precipitation features with different sizes over (a) tropical (20°S–20°N) land, (b) tropical ocean, (c) central Africa, (d) the east Pacific, (e) the Amazon, and (f) the west Pacific (color fill). The percent of LH contribution from convective precipitation is overlaid with contours (in %). Only PFs with at least four pixels are used in this analysis. The location boxes for central Africa, Amazon, the east Pacific, and the west Pacific are shown in Fig. 1c.

rain process. Note that the TRMM PR misses a large proportion of shallow and weak precipitation in the tropics, so the amplitude of this shallow mode is very likely underestimated in Figs. 3d and 3e. MCSs contribute virtually all of the high-altitude LH (95% above 7 km; Table 1) over tropical oceans, both from convective and stratiform precipitation (Figs. 3e,f). However, Fig. 3 only shows the average vertical contribution in the tropics. There are large regional differences in the LH contribution by large organized systems at different levels. For example, the PFs with size greater than 10 000 km^2 contribute a larger proportion of LH at high altitudes (7–8 km) over central Africa than over either the Amazon or the Maritime Continent (region of Indonesia), and more over the east Pacific ITCZ than the west Pacific (Fig. 4a). More than half of the shallow LH at

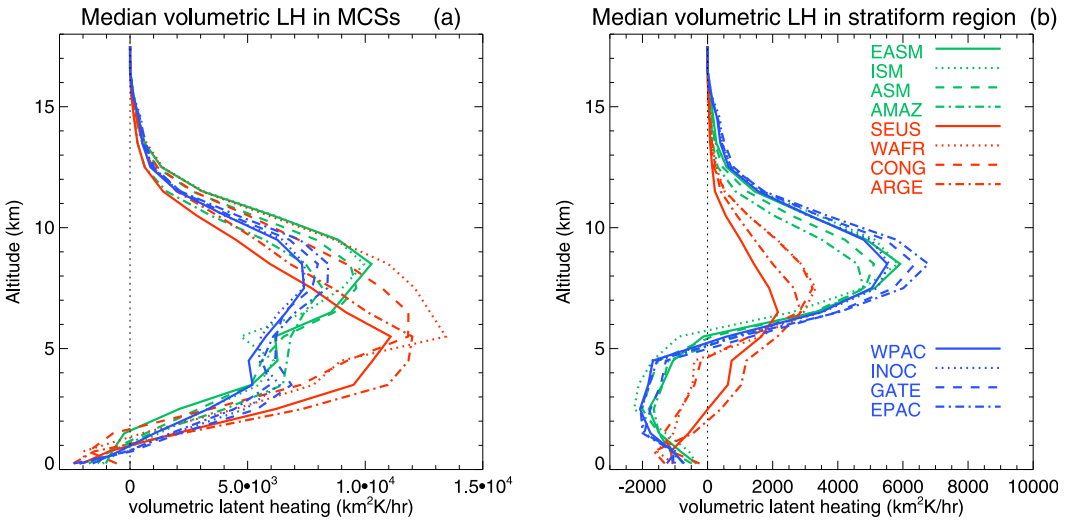

FIG. 6. (a) Median instantaneous volumetric LH in MCSs (PFs > 2000 km^2) during rainy seasonal of regions of interest (Fig. 1c and Table 1). (b) As in (a), but for median volumetric LH from stratiform precipitation. Note that there is an unrealistic positive LH at levels warmer than freezing (~4.5 km) in MCSs over the United States and Argentina. This could be a potential problem in the current version 7 SLH product.

2–5 km is from large PFs over central Africa, which is much higher than the Amazon and the Maritime Continent. At the latitudes poleward of 25°N and 25°S, the large PFs contribute a large proportion of LH at all levels, especially over oceans. Many of those PFs are associated with midlatitude frontal systems during the winter (not shown).

The spectra of fractional contributions of the LH from PFs of various sizes at different altitudes are shown with color fill and percent from convective precipitation are shown with contours in Fig. 5. Consistent with Figs. 3a and 3c, tropical land has one LH mode at 4–8 km mainly from PFs with size greater than 10 000 km^2 (Fig. 5a). Tropical ocean has two LH modes at 1–3 km from small PFs and 6–9 km from large PFs (Fig. 5b). In general, smaller PFs contribute to lower-level LH over both land and ocean. The fraction of convective LH is larger over land than over ocean from PFs with similar size. The fraction of LH from convective precipitation at high altitudes (>6 km) decreases with larger PFs. At the same time, the depth of cooling near the surface due to evaporation increases for larger PFs. The budget of LH from PFs of different sizes varies with regions. For example, the LH contribution from large PFs over central Africa maximizes at slightly lower altitudes (5–7 km; Fig. 5c) than those over the Amazon (6–8 km in Fig. 5e). This is partially due to higher convective LH fraction from PFs in central Africa and a larger proportion of

TABLE 2. Fraction of precipitation, stratiform precipitation, and stratiform LH from mesoscale convective systems (PFs > 2000 km^2) in several tropical and subtropical regions (see Fig. 1) during their rainy seasons.

Region	Season	Type	Percent of rain from MCSs (>2000 km^2)	Percent of stratiform precipitation in MCSs	Percent of LH at 7–10 km from stratiform region
East Asian monsoon region(EASM)	JJA	Monsoon	79	55	77
Indian monsoon region (ISM)	JJA	Monsoon	76	48	76
Asian monsoon region (ASM)	DJF	Monsoon	79	51	75
Amazon (AMAZ)	DJF	Monsoon	76	54	79
Southeastern United States (SEUS)	JJA	Land	72	39	46
Tropical west Africa (WAFR)	JJA	Land	84	41	52
Congo (CONG)	MAM	Land	77	43	58
Agentina (ARGE)	DJF	Land	86	44	51
Western Pacific (WPAC)	JJA	Ocean	77	57	85
Indian Ocean (INOC)	JJA	Ocean	74	54	88
Central Atlantic (GATE)	JJA	Ocean	79	56	87
Eastern Pacific (EPAC)	JJA	Ocean	81	58	87

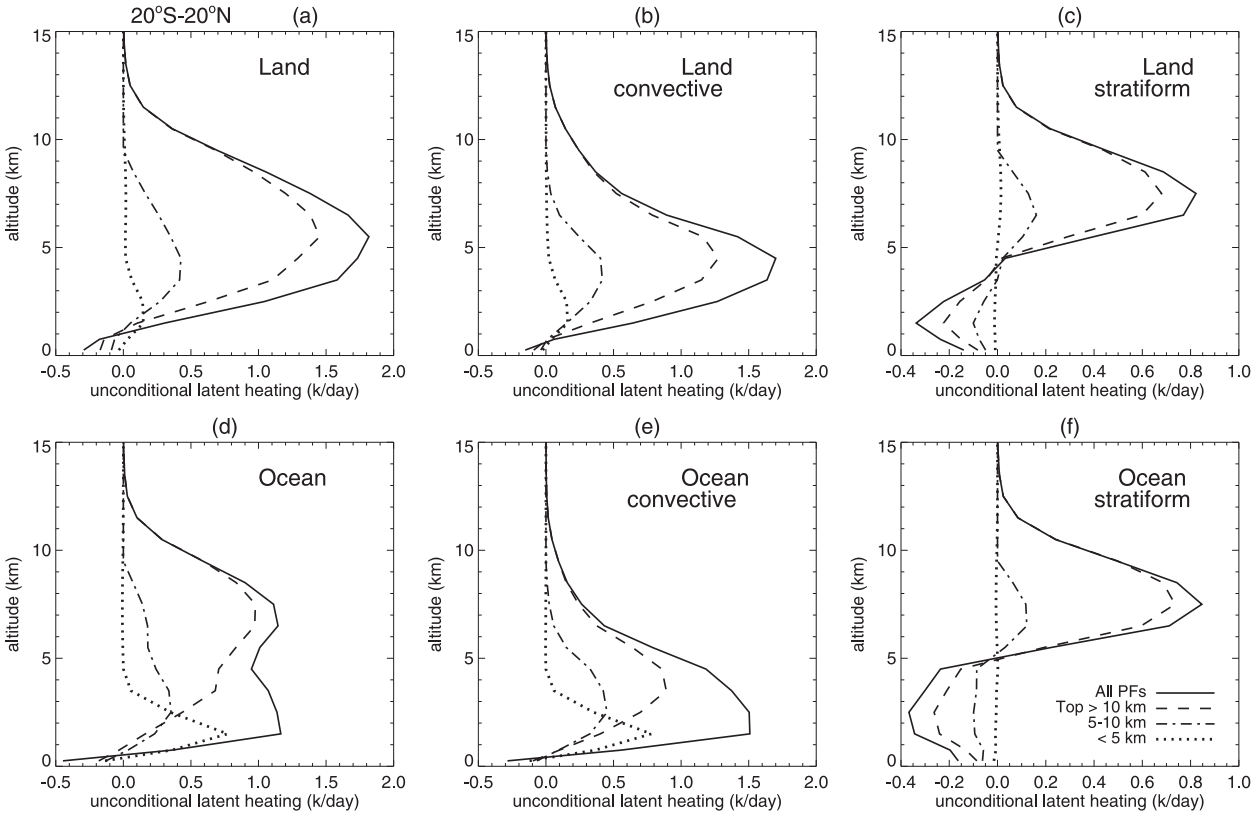

FIG. 7. (a) Mean unconditional LH and contribution from the precipitation features with different depths over tropical (20°S–20°N) land. (b) As in (a), but for LH from the convective precipitation in PFs. (c) As in (a), but for LH from stratiform precipitation in PFs. (d)–(f) As in (a)–(c), but for tropical ocean.

stratiform LH in the Amazon, leading to relatively stronger heating at higher altitudes over the Amazon. Also note that small PFs ($<1000\,km^2$) over central Africa have latent heating at relatively higher altitudes (3–6 km) than those over the Amazon (2–4 km). The LH budget also varies over different ocean basins. Although in general the large PFs have similar LH contributions over the east Pacific and the west Pacific (slightly larger over the west Pacific), the LH contribution from small PFs ($<1000\,km^2$) over the east Pacific is obviously larger. This is probably due to some shallow but organized precipitation systems within the shallow meridional circulation over the east Pacific (Zhang et al. 2004; Liu and Zipser, 2013; Yokoyama et al. 2014).

What causes the regional variations of LH vertical structures? Apparently, abundant small PFs with warm rain have an important contribution to the shallow LH over the ocean. Because large organized MCSs dominate the LH contribution at high altitudes over the rainy regions (Figs. 3–5), the vertical structure of the LH can also be largely influenced by the different properties of MCSs. For example, Fig. 6a shows the median profiles of volumetric LH (sum of LH within PF) at different vertical levels from MCSs over various regions during the rainiest 3 months (Table 2). The continental MCSs (red curves) have LH peaks at relatively lower altitudes (5–6 km) with greater LH volume than those over ocean (8–9 km, blue curves). One main reason for these differences is the fraction of stratiform precipitation. As listed in Table 2, in agreement with Schumacher and Houze (2003), oceanic MCSs have a larger fraction of stratiform precipitation than those over land. The median LH volumes in stratiform regions of oceanic MCSs are also larger than those over land (Fig. 6b). Because the LH in stratiform regions has a top-heavy structure, oceanic MCSs tend to have their LH peak at higher altitudes than MCSs over land. The monsoonal MCSs (green curves) have a top-heavy LH structure similar to oceanic MCSs, with the magnitude of LH in between continental and oceanic MCSs (Table 2, Fig. 6). Note that there is an apparently unrealistic positive LH at levels below 5 km in MCSs over the United States and Argentina. This contradicts the expected evaporative cooling at low levels in the stratiform precipitation region. We recognize that these profiles over land pose a potential problem in the current version 7 SLH

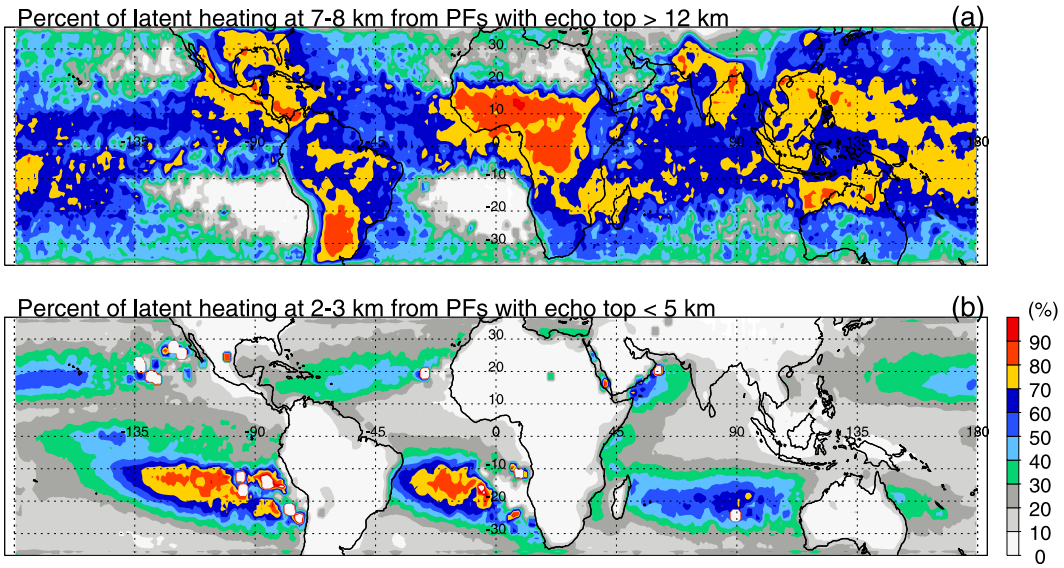

FIG. 8. (a) Percent of LH contribution at 7–8-km level from the precipitation features with echo top greater than 12 km. (b) Percent of LH contribution at 2–3-km level from the precipitation features with echo top less than 5 km.

product and we are currently working on an improved version.

c. *Contribution from precipitation systems with different depths*

Vertical distribution of LH is also directly tied to the depth of the precipitation systems. In the tropics, based on the depth, there are in general three types of convective clouds: shallow cumulus, congestus, and cumulonimbus (Johnson et al. 1999; Wall et al. 2013). Figure 7 shows the LH contributions from PFs with shallow, deep, and midlevel radar echo tops over tropical land and ocean. Deep PFs with echo top greater than 10 km have the largest contributions to the LH at all levels above 2 km over both tropical land and ocean (Table 1, Figs. 7a,d). Since the convective LH dominates over tropical land (Fig. 5a), the deeper convection leads to LH peaks at higher altitudes (Fig. 7b). By definition, the deep stratiform precipitation is entirely associated with deep convection (Figs. 7c,f). Therefore, the deep PFs contribute nearly all the LH above 8 km (Figs. 7a,d). Over tropical oceans, shallow PFs with pure convective precipitation have a significant contribution to LH at low levels (Figs. 7d,e). The PFs with echo top above 5 km have two peaks of LH dominated by the convective and stratiform components separately (Figs. 7d–f). The PFs with echo tops at midlevels do not have a significant contribution at any vertical level, but they do have about 1/3 of LH contribution at 2–5 km over the ocean (Fig. 7d, Table 1).

The geographical distribution of the fractional LH contributions from deep (echo top >12 km) and shallow PFs (echo top <5 km) are shown in Fig. 8. Although in general deep PFs dominate the LH at 7–8 km in the tropics, the fractional contribution varies from 60% to 90% over different regions (Fig. 8a). Over land, deep PFs dominate the LH at 7–8 km over Africa and Argentina (>80%), but only contribute about 60%–70% over the Amazon. Over ocean, deep convection contributes a higher fraction of LH at 7–8 km over the west Pacific warm pool region than over the east and central Pacific and Indian Ocean. Shallow PFs contribute a significant proportion of shallow LH over regions with large-scale descent and dominated by warm rainfall (Liu and Zipser 2009).

The full spectra of LH contributions from PFs of different depths are shown in Fig. 9. The PFs with echo tops reaching 15 km contribute significantly over both tropical land and ocean. These PFs have a stronger peak of LH at lower altitudes (4–7 km) over land (Fig. 9a), and relatively weaker peak of LH at higher altitudes (6–8 km) over ocean (Fig. 9b). This is likely due to the larger fraction of convective precipitation over land and the larger fraction of stratiform precipitation over the oceans. LH above 8 km is mainly from stratiform precipitation for PFs with echo tops below 14 km. However, a large proportion of LH is from convective precipitation when PFs have echo top above 15 km, especially over land. The PFs with echo top above 15 km are likely in the early stage of deep convection that has strong updrafts and has not developed a large area of stratiform precipitation yet. Therefore, the convective precipitation is dominant in these PFs. Consistent with Fig. 8a, deep PFs contribute more LH over Africa than

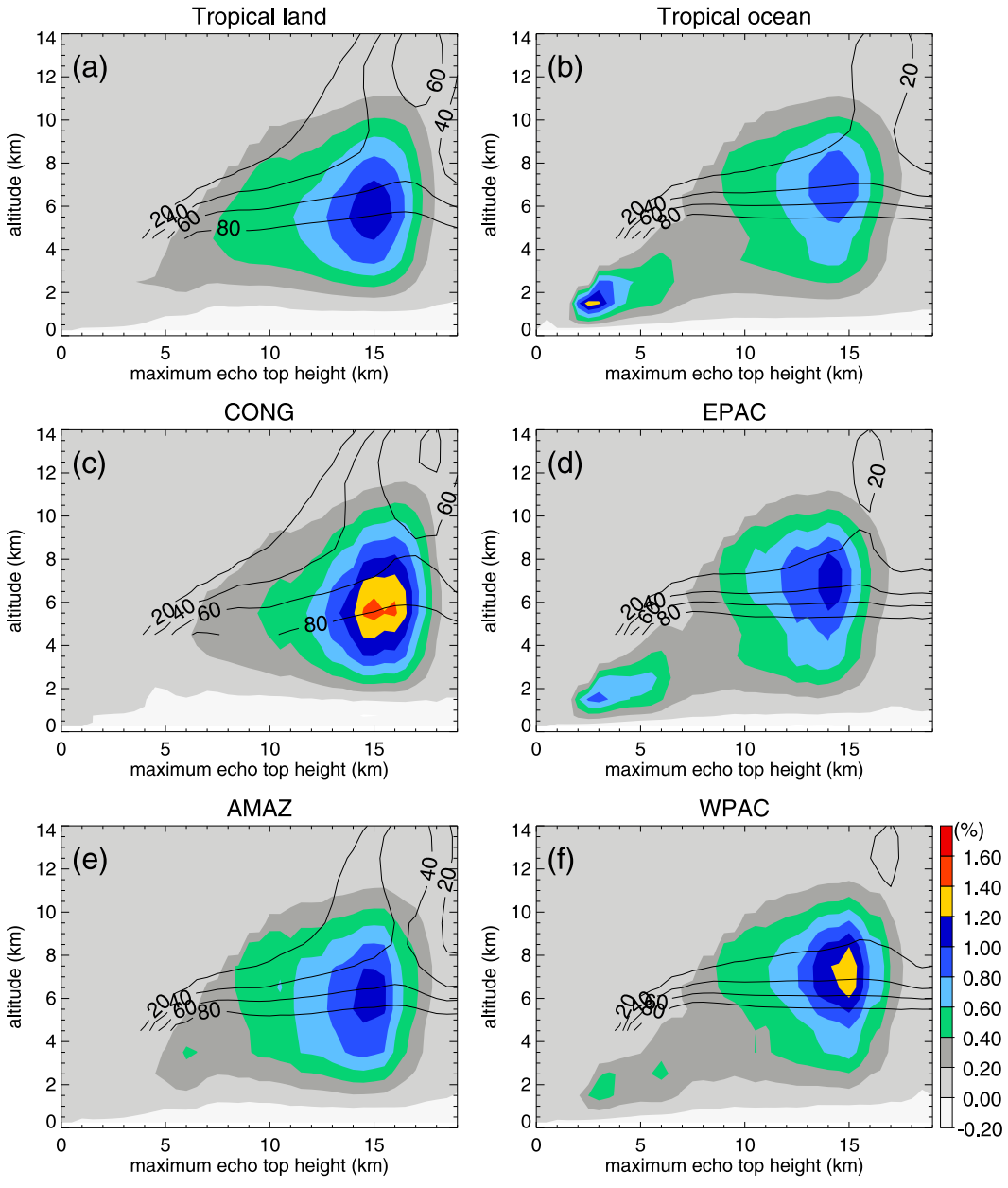

FIG. 9. Fractional contribution of LH at different altitudes from precipitation features with different depths, indicated by the maximum radar echo-top height, over (a) tropical (20°S–20°N) land, (b) tropical ocean, (c) central Africa, (d) the east Pacific, (e) the Amazon, and (f) the west Pacific (color fill). The percent of LH contribution from regions with convective precipitation in these precipitation features is overlaid with contours (in %).

over the Amazon (Figs. 9c,e). There is a larger proportion of convective LH from PFs with echo tops above 15 km over Africa than over the Amazon. It is interesting that there is a small peak of LH at 3–4 km from PFs with echo tops around 6 km over the Amazon. This is consistent with a large population of congestus over the Amazon region (Wall et al. 2013). Comparing the east and west Pacific, the shallow LH from shallow PFs is more important over the east Pacific than over the west Pacific (Figs. 9d,f). The deep PFs contribute a larger proportion of LH at high altitudes over the west Pacific than the east Pacific. The contribution of the congestus is relatively weaker than the deep and shallow PFs over the oceans. However, the trimodal LH contributions from PFs of shallow, deep and midlevel seem to be discernable over the ocean, especially over the west Pacific (Fig. 9f).

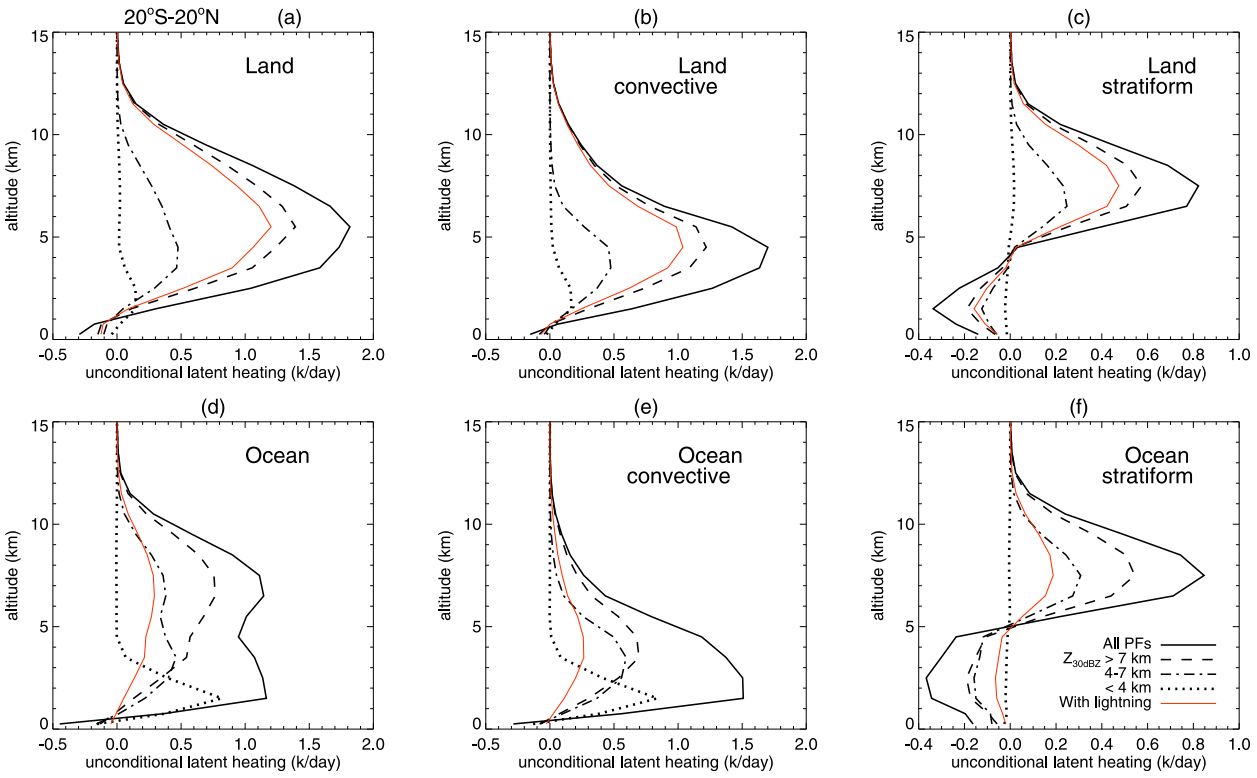

FIG. 10. (a) Mean unconditional LH and contribution from the precipitation features with different convective intensities indicated by maximum height of 30-dBZ PR reflectivity over tropical (20°S–20°N) land. The contributions from the thunderstorms are also shown with red curve. (b) As in (a), but for LH from the convective precipitation in PFs. (c) As in (a), but for LH from stratiform precipitation in PFs. (d)–(f) As in (a)–(c), but for tropical ocean.

d. Contribution from precipitation systems with different convective intensities

The vertical distribution of LH may also be modulated by the intensity of convection. For example, the strength of convective updrafts may affect the altitude/temperature levels where raindrops freeze (Zipser 2003), which in turn may influence updraft strength in the upper troposphere. Also, precipitation systems have different convective intensities during their life cycles. For example, a MCS usually has stronger updrafts in its early and mature stage than its dissipation stage. Therefore, the study of LH from PFs with different convective intensity may also help understanding the variation of LH during the life cycles of precipitation systems.

Figure 10 shows the LH contribution from PFs with different 30-dBZ heights. Because radar reflectivity is sensitive to the size of the hydrometeors, 30-dBZ radar reflectivity in the mixed phase levels may be used as a proxy for the presence of large ice particles and even a good indicator of lightning (Liu et al. 2012). Strong PFs with 30-dBZ tops greater than 7 km and thunderstorms (PFs with lightning) contribute a major proportion of the LH at all levels above 2 km over tropical land (Table 1, Fig. 10a). Over tropical oceans, the small (Fig. 3d), shallow (Fig. 7d), and weak (Fig. 10d) PFs contribute to most of the shallow LH, while strong PFs with 30-dBZ height above 7 km contribute a big proportion of LH at high altitudes. Although it is rare to have lightning over tropical oceans, the thunderstorms over ocean usually have a large horizontal extent (e.g., Fig. 5b of Cecil et al. 2005) and contribute a noticeable proportion (>25%) of LHs at high altitudes (Table 1). While the LH contributions from PFs with lightning over land have very similar vertical structure (e.g., peak level), with PFs with tall convection (Figs. 10a,b), it is not the same for PFs over the oceans (Figs. 10d,e). This is consistent with the findings of Takayabu (2006), who showed a significant correlation between the rainfall-relative lightning frequency and tall rainfall contributions only over land but not over the oceans. Clarifying differences in lightning systems over land versus oceans is an interesting topic but left for future studies.

Because the most intense convection mainly occurs over land (Zipser et al. 2006), the LH contribution from these intense PFs is larger over land, especially over the Congo basin, Sahel, Argentina, Pakistan, and the Great

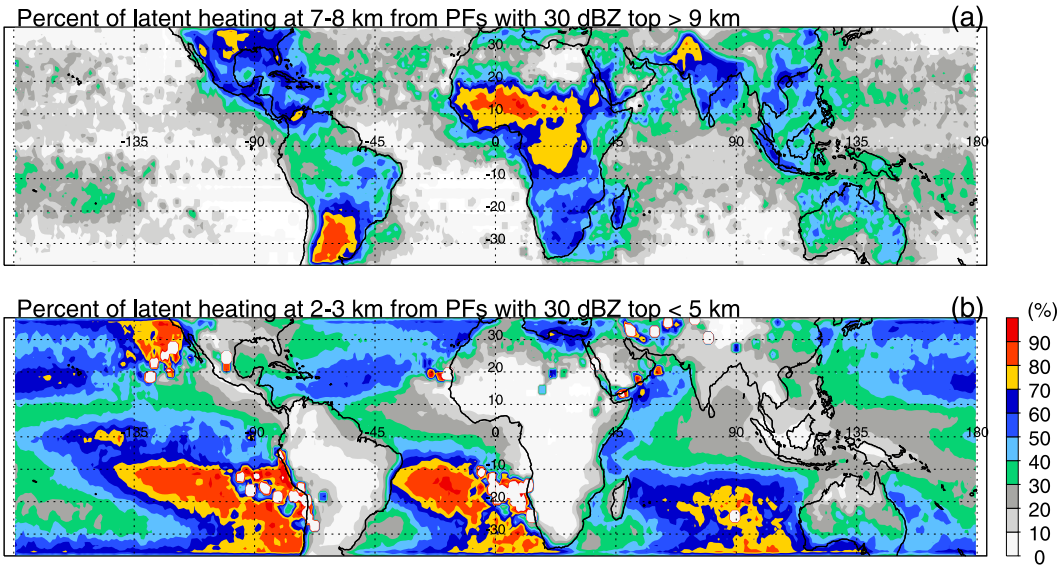

FIG. 11. (a) Percent of LH contribution at 7–8-km level from the precipitation features with maximum 30-dBZ height greater than 9 km. (b) Percent of LH contribution at 2–3-km level from the precipitation features with maximum 30-dBZ height less than 5 km. Note that white inside red are actually values above the maximum values shown on the color scale.

Plains of the United States (Fig. 11a). Weak PFs contribute most of the shallow LH over oceanic regions with a large-scale descent (Fig. 11b). Over the east central Pacific, equatorial PFs with weaker convection contribute up to 80% of shallow heating, compared with 20%–30% over other equatorial oceans. Over land, PFs with weaker convection contribute around 30%–40% of shallow LH over east China, compared with much lower contributions over other continental regions. Some of these PFs may be associated with the mei-yu front characterized with abundant warm rain (Xu et al. 2009).

Full spectra of LH contribution from PFs with different 30-dBZ top heights are shown in Fig. 12. PFs with 30-dBZ echo top at 5–9 km contribute a large proportion of LH over both land and ocean. However, these PFs have a stronger contribution at lower altitudes over land (3–7 km) than over ocean (5–9 km). Because of the relatively weak convection, there is a minimum contribution of LH from PFs with 30-dBZ echo top greater than 10 km over ocean (Fig. 12b). Consistent with Fig. 10d, weak PFs have a very large contribution to shallow LH over ocean. One interesting feature in Figs. 12a and 12b is that the convective fraction of LH above 7 km becomes a minimum when PFs have 30-dBZ echo top between 5 and 9 km, and increases with higher 30-dBZ tops. We speculate that the strong PFs with 30-dBZ top above 9 km are at an early stage of their life cycles and therefore have a higher fraction of convective precipitation. It then follows that most of the PFs with 30-dBZ tops at 5–9 km are at their mature or dissipation stages and have developed a large volume of stratiform precipitation, and therefore have a more top-heavy LH structure.

Because the convective intensity changes from one place to another, there are large variations among the spectrum of LH from PFs of different 30-dBZ heights over different regions. For example, strong PFs with 30-dBZ top above 9 km have a much larger contribution to the LH over Africa (Fig. 12c) than over the Amazon (Fig. 12e). Convective systems over the "green ocean" Amazon region (Silva Dias et al. 2002) have many characteristics close to oceanic precipitation systems. As a result, the spectrum of LH contribution from PFs of different intensity over the Amazon (Fig. 12e) looks more like oceanic PFs (Fig. 12b) than the continental PFs (Fig. 12a). Comparing the east Pacific and the west Pacific, weak PFs with 30-dBZ top below 4 km over the east Pacific have larger shallow LH contributions (Fig. 12d). Relatively intense PFs with 30-dBZ top above 5 km have larger contributions of deep LH over the west Pacific versus the east Pacific (Fig. 12f).

e. Diurnal variation of LH

There is a long history of studies on the diurnal variations of clouds and precipitation (Gray and Jacobson 1977; Augustine 1984; Hall and Vonder Haar 1999; Nesbitt and Zipser 2003). In general, clouds and precipitation have a stronger diurnal variation over land with a strong peak in the late afternoon and a weaker diurnal variation over ocean with a slight peak in the

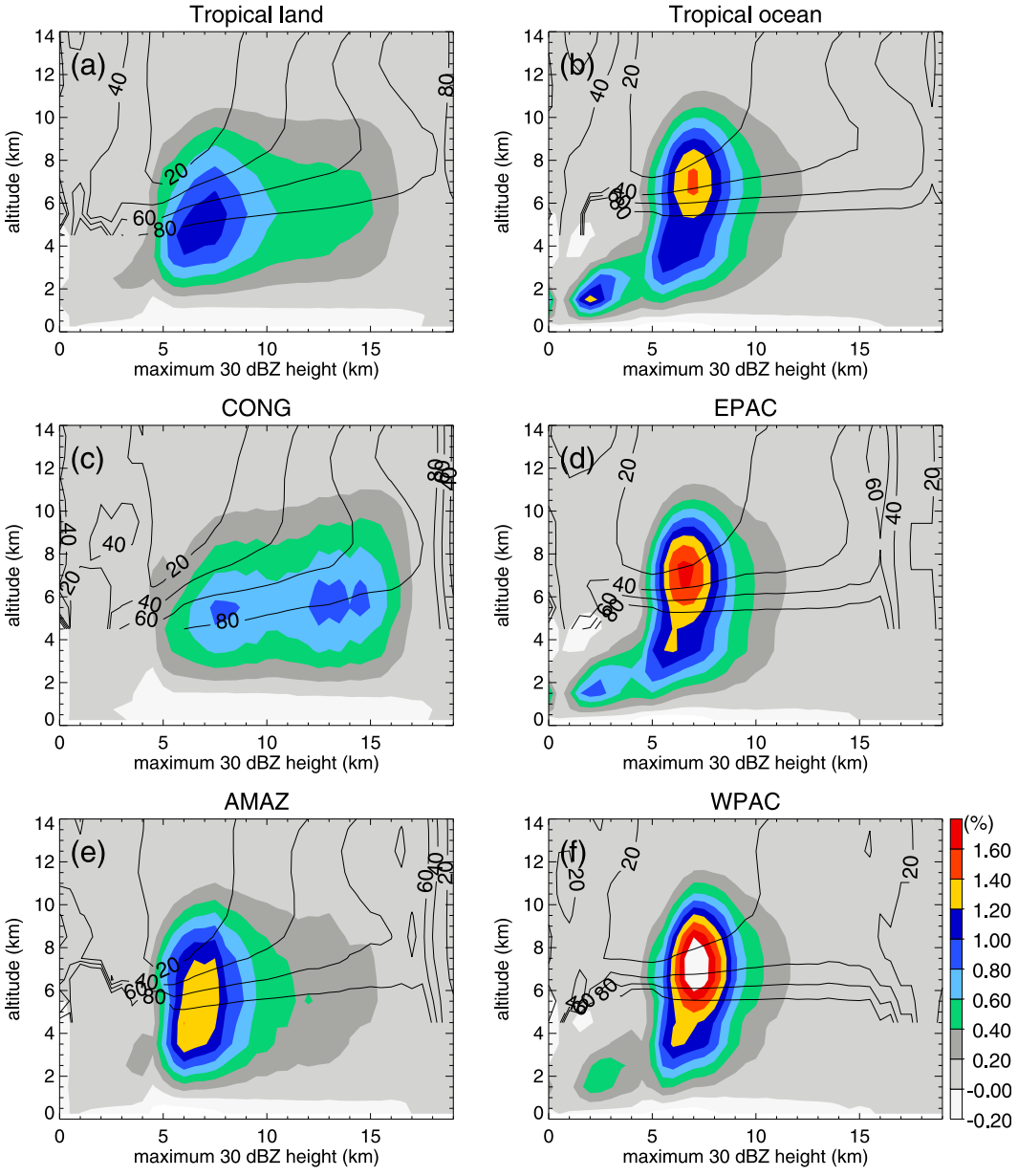

FIG. 12. Fractional contribution of LH at different altitudes from precipitation features with different convective intensities, indicated by the maximum 30-dB*Z* echo-top height, over (a) tropical (20°S–20°N) land, (b) tropical ocean, (c) central Africa, (d) the east Pacific, (e) the Amazon, and (f) the west Pacific (color fill). The percent of LH contribution from regions with convective precipitation in these precipitation features is overlaid with contours (in %). Note that white inside red are actually values above the maximum values shown on the color scale.

early morning. The diurnal change of clouds and precipitation is directly related to precipitation systems of different types and life cycles. Not only would the total LH change with the total precipitation diurnally, but the vertical distribution of LH would shift diurnally because some types of precipitation systems tend to occur or be at certain stage of life cycles during specific local times over different regions. This has been confirmed from field campaign observations (Schumacher et al. 2007).

Diurnal variation of unconditional LH over tropical land and ocean from 15 years of SLH retrievals are shown in Fig. 13. Consistent with the diurnal variation of precipitation, LH is much stronger in the later afternoon between 1300 and 1800 LT over land (Fig. 13a) and is slightly stronger in the early morning between 0200 and 0700 LT over ocean (Fig. 13b). Further, there are some interesting details in the variations of LH vertical distributions. Over land, there is a tilted structure of LH in

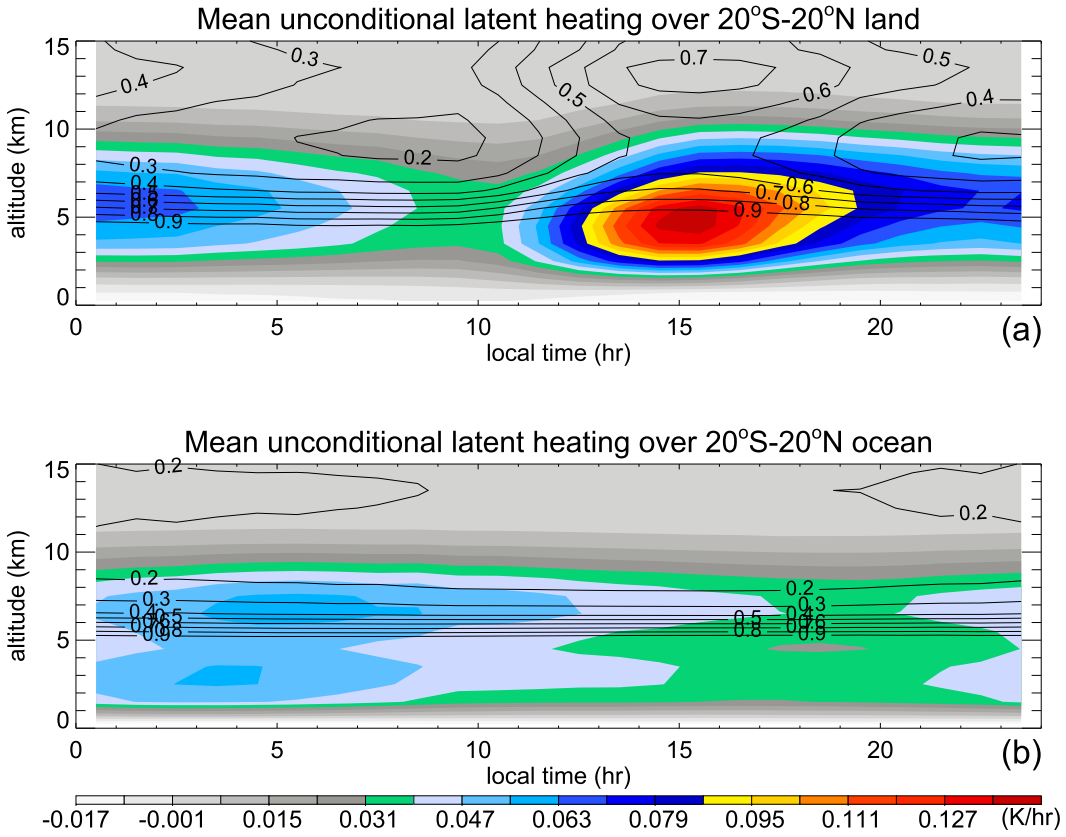

FIG. 13. (a) Diurnal variation of mean unconditional LH (color fill) and the fractional contribution (contours) from convective precipitation over tropical land. (b) As in (a), but for over tropical ocean.

the late afternoon with relatively shallower LH at 4–6 km in the early afternoon and deeper LH at 5–7 km in the late afternoon. In the early afternoon, convective systems tend to be at an early developing stage and mainly consist of convective precipitation (Fig. 13a). Convective LH even dominates the LH at high altitudes at this stage (contours in Fig. 13a). Therefore, the LH is relatively shallow due to the bottom-heavy structure of convective LH. In the late afternoon and early evening, some convective systems develop and become MCSs with a large volume of stratiform precipitation. With a top-heavy LH of stratiform precipitation, the LH profile is relatively deeper. Then these large MCSs could keep developing till the early morning and dissipate with a deep LH structure (Fig. 13a). Over ocean, shallow and deep LH modes have slightly different diurnal variations (Fig. 13b). Shallow LH peaks earlier than the deep LH in the early morning. Abundant small, shallow, and weak precipitation systems contribute to most of the shallow LH and are most frequent in the early morning. MCSs tend to occur at all local times over ocean with a slight preference for the early morning hours. The stratiform LH dominates above 7 km at all times over ocean.

Figure 14 shows the unconditional LH from convective precipitation only, with the fractional LH contribution from MCSs superimposed. Over tropical land, convective LH dominates in the afternoon between 1300 and 1800 LT. MCSs contribute virtually all of the LH especially at high altitudes above 5 km, except in the afternoon between 1300 and 1800 LT when smaller convective systems have some contribution at high altitudes as well (e.g., 20%–30% at 7–9 km) (Fig. 14a). Over ocean, without the LH from stratiform precipitation, the deep LH mode shown in Fig. 13b can no longer be seen for convective LH (Fig. 14b). Also over ocean, Fig. 14b demonstrates that convective heating once again peaks at low altitudes (1–4 km), in contrast to Fig. 13b. The main reason is that Fig. 14b no longer includes the cooling at low levels from evaporation of rain in stratiform precipitation from MCSs that is included in Fig. 13b. MCSs have similar contribution of LH at all local times over ocean.

4. Summary and discussion

Using 15 years of TRMM Spectral Latent Heating (SLH) products, the horizontal and vertical distribution

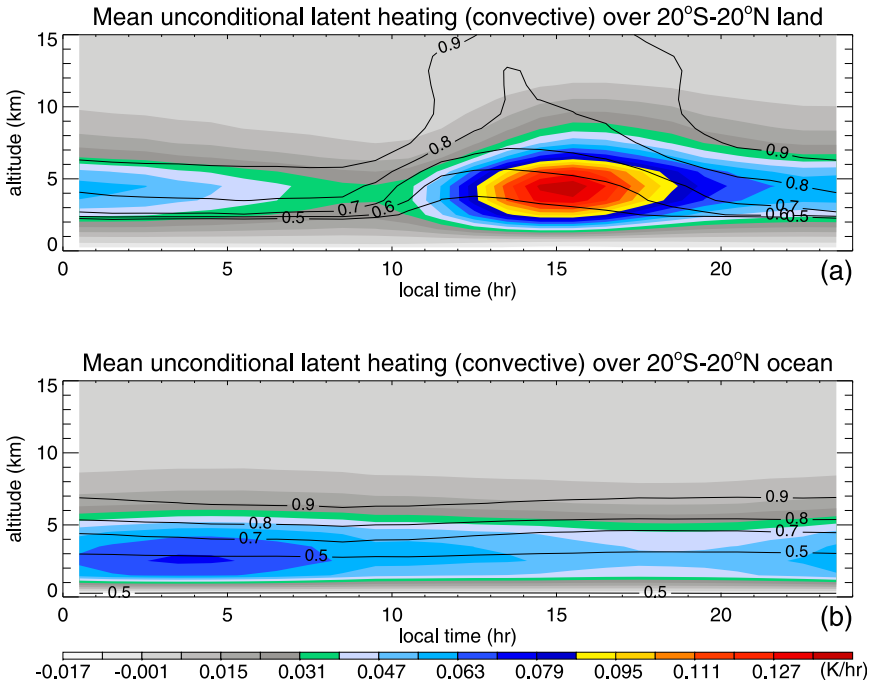

FIG. 14. (a) Diurnal variation of mean unconditional LH from convective precipitation (color fill), and the fractional contribution of total unconditional LH (contours) from MCSs (area > 2000 km^2) derived from precipitation features over tropical land. (b) As in (a), but for over tropical ocean.

of LH contributed by precipitation systems of different size, depth, and intensity is analyzed between 36°N and 36°S. The major findings include the following:

- Over both land and ocean, large, deep, organized mesoscale convective systems (MCSs) contribute most of the LH, especially in the upper troposphere, where the MCS contribution may approach 100%. Over tropical land, convective LH exceeds stratiform LH, with the combined LH peak in the 4–7-km altitude range. Over tropical ocean, there is a double peak in LH, with the lower peak mainly contributed by small shallow precipitation features and the upper peak from MCSs. Over tropical oceans, stratiform LH and convective LH are similar in magnitude, with the large stratiform component contributing greatly to the peak above 7-km altitude.
- Regional and seasonal variations of the vertical profile of LH are linked to the relative proportions of different types of precipitation systems. One clear example is found in the subtropical oceans where small, shallow precipitation features are dominant, with a latent heating peak in the 1–3-km range. These can be mostly stratocumulus in inversion-dominated regions but can also be shallow cumulus, especially closer to the deep tropics.

Larger convective systems such as MCSs have larger stratiform fractions over tropical oceans but smaller stratiform fractions over continents, especially over regions with more intense convection (the United States, Argentina, Africa). In general, the larger the stratiform fraction, as over tropical oceans, the more dominant is the upper tropospheric LH peak. Monsoonal MCSs have properties intermediate between those of continental and oceanic MCSs.

- There are significant differences in LH profiles over land from one region to another, and many of these differences seem to be linked to the different intensity of convection, or the differences in size of MCSs, or both. There are clear differences between the Amazon and Africa, and between monsoon regions and subtropical regions known for very intense convection, such as the central United States and southeastern South America,
- Although three modes of convection (shallow, congestus, and deep) are detected over tropical oceans, the LH contribution from congestus is small and seems to vary from one ocean basin to another.
- Consistent with the diurnal variation of precipitation, LH varies much more strongly over land, with a strong afternoon maximum, than over ocean, with a very broad night and morning maximum. The afternoon maximum over land has a significant contribution by smaller convective systems, whereas large MCSs are

dominant at all other times. The shallow mode of LH over oceans maximizes somewhat earlier than the deep mode in the early morning.

In the future, it will be important to use these results to develop improvements to the SLH algorithm. In particular, the suite of look-up tables currently in use is based upon data obtained from a limited number of field programs. These datasets are probably more representative of tropical oceans than they are over tropical and subtropical land. The LH profiles have been shown to be sensitive to the intensity and depth of the convection, and to the size and structure of MCSs. Different continental regions with characteristically different convective intensity should be considered for development of look-up tables matched to conditions in each region. The results could also be used to test how well global climate models capture LH profiles of various organized precipitation systems.

Acknowledgments. The authors benefited from discussions with Dr. Robert Houze. The constructive comments of the three reviewers are appreciated and improved the clarity and readability of the manuscript. This research was supported by NASA Precipitation Measurement Mission Grants NNX13AF73G and NNX11AG31G under the direction of Dr. Ramesh Kakar and NASA Grant NNX08AK28G under the direction of Dr. Erich Stocker. Thanks also go to Drs. Erich Stocker and John Kwiatkowski and the rest of the Precipitation Processing System (PPS) team at NASA Goddard Space Flight Center, Greenbelt, MD, for data processing assistance.

REFERENCES

Arakawa, A., 1975: Modelling clouds and cloud processes for use in climate model. *The Physical Basis of Climate and Climate Modelling,* GARP Publication Series, No. 16, WMO, 183–197.

Augustine, J. A., 1984: The diurnal variation of large-scale inferred rainfall over the tropical Pacific Ocean during August 1979. *Mon. Wea. Rev.,* **112,** 1745–1751, doi:10.1175/1520-0493(1984)112<1745:TDVOLS>2.0.CO;2.

Awaka, J., T. Iguchi, and K. Okamoto, 1998: Early results on rain type classification by the Tropical Rainfall Measuring Mission (TRMM) precipitation radar. *Proc. Eighth URSI Commission F Open Symp.,* Aveiro, Portugal, International Union of Radio Science, 143–146.

——, H. Kumagai, and T. Iguchi, 2009: TRMM PR standard algorithm 2A23 and its performance on bright band detection. *J. Meteor. Soc. Japan,* **87A,** 31–52, doi:10.2151/jmsj.87A.31.

Cecil, D. J., S. J. Goodman, D. J. Boccippio, E. J. Zipser, and S. W. Nesbitt, 2005: Three year of TRMM precipitation features. Part I: Radar, radiometric, and lightning characteristics. *Mon. Wea. Rev.,* **133,** 543–566, doi:10.1175/MWR-2876.1.

Del Genio, A. D., 2012: Representing the sensitivity of convective cloud systems to the tropospheric humidity in general circulation model. *Surv. Geophys.,* **33,** 637–656, doi:10.1007/s10712-011-9148-9.

Emanuel, K. E., J. D. Neelin, and C. S. Bretherton, 1994: On large-scale circulations in convecting atmospheres. *Quart. J. Roy. Meteor. Soc.,* **120,** 1111–1143, doi:10.1002/qj.49712051902.

Frank, W. M., and J. L. McBride, 1989: The vertical distribution of heating in AMEX and GATE cloud clusters. *J. Atmos. Sci.,* **46,** 3464–3478, doi:10.1175/1520-0469(1989)046<3464:TVDOHI>2.0.CO;2.

Fu, Y., and G. Liu, 2007: Possible misidentification of rain type by TRMM PR over the Tibetan Plateau. *J. Appl. Meteor. Climatol.,* **46,** 667–672, doi:10.1175/JAM2484.1.

Funk, A., and C. Schumacher, 2013: Analysis of rain classification over the tropics by version 7 of the TRMM 2A23 algorithm. *J. Meteor. Soc. Japan,* **91,** 257–272, doi:10.2151/jmsj.2013-302.

Gray, W. M., and R. W. Jacobson, 1977: Diurnal variation of deep cumulus convection. *Mon. Wea. Rev.,* **105,** 1171–1188, doi:10.1175/1520-0493(1977)105<1171:DVODCC>2.0.CO;2.

Hall, T. J., and T. H. Vonder Haar, 1999: The diurnal cycle of west Pacific deep convection and its relation to the spatial and temporal variation of tropical MCSs. *J. Atmos. Sci.,* **56,** 3401–3415, doi:10.1175/1520-0469(1999)056<3401:TDCOWP>2.0.CO;2.

Houze, R. A., Jr., 1989: Observed structure of mesoscale convective systems and implications for large-scale heating. *Quart. J. Roy. Meteor. Soc.,* **115,** 425–461, doi:10.1002/qj.49711548702.

——, 1997: Stratiform precipitation in regions of convection: A meteorological paradox. *Bull. Amer. Meteor. Soc.,* **78,** 2179–2196, doi:10.1175/1520-0477(1997)078<2179:SPIROC>2.0.CO;2.

——, 2004: Mesoscale convective systems. *Rev. Geophys.,* **42,** RG4003, doi:10.1029/2004RG000150.

Imaoka, K., and K. Nakamura, 2013: Statistical analysis of temporal variation of heating profiles associated with isolated tropical cold cloud systems by using satellite observations. *SOLA,* **9,** 51–55, doi:10.2151/sola.2013-012.

Jakob, C., and C. Schumacher, 2008: Precipitation and latent heating characteristics of the major tropical western Pacific cloud regimes. *J. Climate,* **21,** 4348–4364, doi:10.1175/2008JCLI2122.1.

Johnson, R. H., 1976: The role of convective-scale precipitation downdrafts in cumulus and synoptic-scale interactions. *J. Atmos. Sci.,* **33,** 1890–1910, doi:10.1175/1520-0469(1976)033<1890:TROCSP>2.0.CO;2.

——, 1984: Partitioning tropical heat and moisture budgets into cumulus and mesoscale components: Implications for cumulus parameterization. *Mon. Wea. Rev.,* **112,** 1590–1601, doi:10.1175/1520-0493(1984)112<1590:PTHAMB>2.0.CO;2.

——, T. M. Rickenbach, S. A. Rutledge, P. E. Ciesielski, and W. H. Schubert, 1999: Trimodal characteristics of tropical convection. *J. Climate,* **12,** 2397–2418, doi:10.1175/1520-0442(1999)012<2397:TCOTC>2.0.CO;2.

Kummerow, C., W. Barnes, T. Kozu, J. Shiue, and J. Simpson, 1998: The Tropical Rainfall Measuring Mission (TRMM) sensor package. *J. Atmos. Oceanic Technol.,* **15,** 809–817, doi:10.1175/1520-0426(1998)015<0809:TTRMMT>2.0.CO;2.

Lebsock, M. D., and T. S. L'Ecuyer, 2011: The retrieval of warm rain from CloudSat. *J. Geophys. Res.,* **116,** D20209, doi:10.1029/2011JD016076.

Liu, C., 2011: Rainfall contributions from precipitation systems with different sizes, convective intensities, and durations over the tropics and subtropics. *J. Hydrometeor.,* **12,** 394–412, doi:10.1175/2010JHM1320.1.

——, and E. J. Zipser, 2009: "Warm rain" in the tropics: Seasonal and regional distribution based on 9 years of TRMM data. *J. Climate,* **22,** 767–779, doi:10.1175/2008JCLI2641.1.

——, and ——, 2013: Regional variation of the morphology of organized convection in the tropics and subtropics. *J. Geophys. Res. Atmos.,* **118,** 453–466, doi:10.1029/2012JD018409.

——, ——, D. J. Cecil, S. W. Nesbitt, and S. Sherwood, 2008: A cloud and precipitation feature database from 9 years of TRMM observations. *J. Appl. Meteor. Climatol.,* **47,** 2712–2728, doi:10.1175/2008JAMC1890.1.

——, D. Cecil, and E. J. Zipser, 2012: Relationships between lightning flash rates and radar reflectivity vertical structures in thunderstorms over the tropics and subtropics. *J. Geophys. Res.,* **117,** D06212, doi:10.1029/2011JD017123.

Mapes, B. E., and R. Neale, 2011: Parameterizing convective organization to evade entrainment dilemma. *J. Adv. Model. Earth Syst.,* **3,** M06004, doi:10.1029/2011MS000042.

——, P. E. Ciesielski, and R. H. Johnson, 2003: Sampling errors in rawinsonde-array budgets. *J. Atmos. Sci.,* **60,** 2697–2714, doi:10.1175/1520-0469(2003)060<2697:SEIRB>2.0.CO;2.

Morita, J., Y. N. Takayabu, S. Shige, and Y. Kodama, 2006: Analysis of rainfall characteristics of the Madden–Julian oscillation using TRMM satellite data. *Dyn. Atmos. Oceans,* **42,** 107–126, doi:10.1016/j.dynatmoce.2006.02.002.

Nesbitt, S. W., and E. J. Zipser, 2003: The diurnal cycle of rainfall and convective intensity according to three years of TRMM measurements. *J. Climate,* **16,** 1456–1475, doi:10.1175/1520-0442-16.10.1456.

——, R. Cifelli, and S. A. Rutledge, 2006: Storm morphology and rainfall characteristics of TRMM precipitation features. *Mon. Wea. Rev.,* **134,** 2702–2721, doi:10.1175/MWR3200.1.

Nitta, T., and S. Esbensen, 1974: Heat and moisture budget analysis using BOMEX data. *Mon. Wea. Rev.,* **102,** 17–28, doi:10.1175/1520-0493(1974)102<0017:HAMBAU>2.0.CO;2.

Riehl, H., and J. S. Malkus, 1958: On the heat balance in the equatorial trough zone. *Geophysica,* **6,** 503–538.

Schumacher, C., and R. A. Houze Jr., 2003: Stratiform rain in the tropics as seen by the TRMM precipitation radar. *J. Climate,* **16,** 1739–1756, doi:10.1175/1520-0442(2003)016<1739:SRITTA>2.0.CO;2.

——, ——, and I. Kraucunas, 2004: The tropical dynamical response to latent heating estimates derived from the TRMM precipitation radar. *J. Atmos. Sci.,* **61,** 1341–1358, doi:10.1175/1520-0469(2004)061<1341:TTDRTL>2.0.CO;2.

——, M. H. Zhang, and P. E. Ciesielski, 2007: Heating structures of the TRMM field campaigns. *J. Atmos. Sci.,* **64,** 2593–2610, doi:10.1175/JAS3938.1.

Shige, S., Y. N. Takayabu, W.-L. Tao, and D. E. Johnson, 2004: Spectral retrieval of latent heating profiles from TRMM PR data. Part I: Development of a model-based algorithm. *J. Appl. Meteor.,* **43,** 1095–1113, doi:10.1175/1520-0450(2004)043<1095:SROLHP>2.0.CO;2.

——, ——, ——, and C.-L. Shie, 2007: Spectral retrieval of latent heating profiles from TRMM PR data. Part II: Algorithm improvement and heating estimates over tropical ocean regions. *J. Appl. Meteor. Climatol.,* **46,** 1098–1124, doi:10.1175/JAM2510.1.

——, ——, and ——, 2008: Spectral retrieval of latent heating profiles from TRMM PR data. Part III: Estimating apparent moisture sink profiles over tropical oceans. *J. Appl. Meteor. Climatol.,* **47,** 620–640, doi:10.1175/2007JAMC1738.1.

——, ——, S. Kinda, W.-K. Tao, X. Zeng, C. Yokiyama, and T. L'Ecuyer, 2009: Spectral retrieval of latent heating profiles from TRMM PR data. Part IV: Comparisons of lookup tables from two- and three-dimensional cloud-resolving model simulations. *J. Climate,* **22,** 5577–5594, doi:10.1175/2009JCLI2919.1.

Silva Dias, M. A. F., and Coauthors, 2002: Cloud and rain processes in a biosphere–atmosphere interaction context in the Amazon region. *J. Geophys. Res.,* **107,** 8072, doi:10.1029/2001JD000335.

Simpson, J., R. F. Adler, and G. R. North, 1988: Proposed Tropical Rainfall Measuring Mission (TRMM) satellite. *Bull. Amer. Meteor. Soc.,* **69,** 278–295, doi:10.1175/1520-0477(1988)069<0278:APTRMM>2.0.CO;2.

Takayabu, Y. N., 2006: Rain-yield per flash calculated from TRMM PR and LIS data and its relationship to the contribution of tall convective rain. *Geophys. Res. Lett.,* **33,** L18705, doi:10.1029/2006GL027531.

——, S. Shige, W.-K. Tao, and N. Hirota, 2010: Shallow and deep latent heating modes over tropical oceans observed with TRMM PR spectral latent heating data. *J. Climate,* **23,** 2030–2046, doi:10.1175/2009JCLI3110.1.

Tao, W.-K., and Coauthors, 2006: Retrieval of latent heating from TRMM measurements. *Bull. Amer. Meteor. Soc.,* **87,** 1555–1572, doi:10.1175/BAMS-87-11-1555.

——, S. Lang, X. Zeng, S. Shige, and Y. Takayabu, 2010: Relating convective and stratiform rain to latent heating. *J. Climate,* **23,** 1874–1893, doi:10.1175/2009JCLI3278.1.

Thompson, R. M., Jr., S. W. Payne, E. E. Rechker, and R. J. Reed, 1979: Structure and properties of synoptic-scale wave disturbances in the intertropical convergence zone of the eastern Atlantic. *J. Atmos. Sci.,* **36,** 53–72, doi:10.1175/1520-0469(1979)036<0053:SAPOSS>2.0.CO;2.

Wall, C., C. Liu, and E. J. Zipser, 2013: A climatology of tropical congestus using CloudSat. *J. Geophys. Res. Atmos.,* **118,** 6478–6492, doi:10.1002/jgrd.50455.

Xu, W., E. J. Zipser, and C. Liu, 2009: Rainfall characteristics and convective properties of mei-yu precipitation systems over south China and Taiwan, Part I: TRMM observations. *Mon. Wea. Rev.,* **137,** 4261–4275, doi:10.1175/2009MWR2982.1.

Yanai, M., and R. H. Johnson, 1993: Impacts of cumulus convection on thermodynamic fields. *The Representation of Cumulus Convection in Numerical Models, Meteor. Monogr.,* No. 46, Amer. Meteor. Soc., 39–62.

——, S. Esbensen, and J.-H. Chu, 1973: Determination of bulk properties of tropical cloud clusters from large-scale circulation in the tropics. *J. Atmos. Sci.,* **30,** 611–627, doi:10.1175/1520-0469(1973)030<0611:DOBPOT>2.0.CO;2.

Yokoyama, C., E. J. Zipser, and C. Liu, 2014: TRMM-observed shallow vs. deep convection in the eastern Pacific related to large-scale circulations in reanalysis datasets. *J. Climate,* **27,** 5575–5592, doi:10.1175/JCLI-D-13-00315.1.

Zhang, C., M. McGauley, and N. A. Bond, 2004: Shallow meridional circulation in the tropical eastern Pacific. *J. Climate,* **17,** 133–139, doi:10.1175/1520-0442(2004)017<0133:SMCITT>2.0.CO;2.

——, and Coauthors, 2010: MJO signals in latent heating: Results from TRMM retrievals. *J. Atmos. Sci.,* **67,** 3488–3508, doi:10.1175/2010JAS3398.1.

Zipser, E. J., 2003: Some views on ''hot towers'' after 50 years of tropical field programs and two years of TRMM data. *Cloud Systems, Hurricanes, and the Tropical Rainfall Measuring Mission, Meteor. Monogr.,* No. 51, Amer. Meteor. Soc., 49–58, doi:10.1175/0065-9401(2003)029<0049:CSVOHT>2.0.CO;2.

——, C. Liu, D. Cecil, S. W. Nesbitt, and S. Yorty, 2006: Where are the most intense thunderstorms on Earth? *Bull. Amer. Meteor. Soc.,* **87,** 1057–1071, doi:10.1175/BAMS-87-8-1057.